CHAPTER II

THEORY

2.1 Molecular Sieves

In 1932, McBain proposed a term "molecular sieve"[38] to describe a number of materials that exhibit selective adsorption properties due to their porous structure. A material that can be a molecular sieve, must separate a mixture of components on the basis of molecular size and shape differences. The different classes of molecular sieve materials are listed in Figure 2.1.

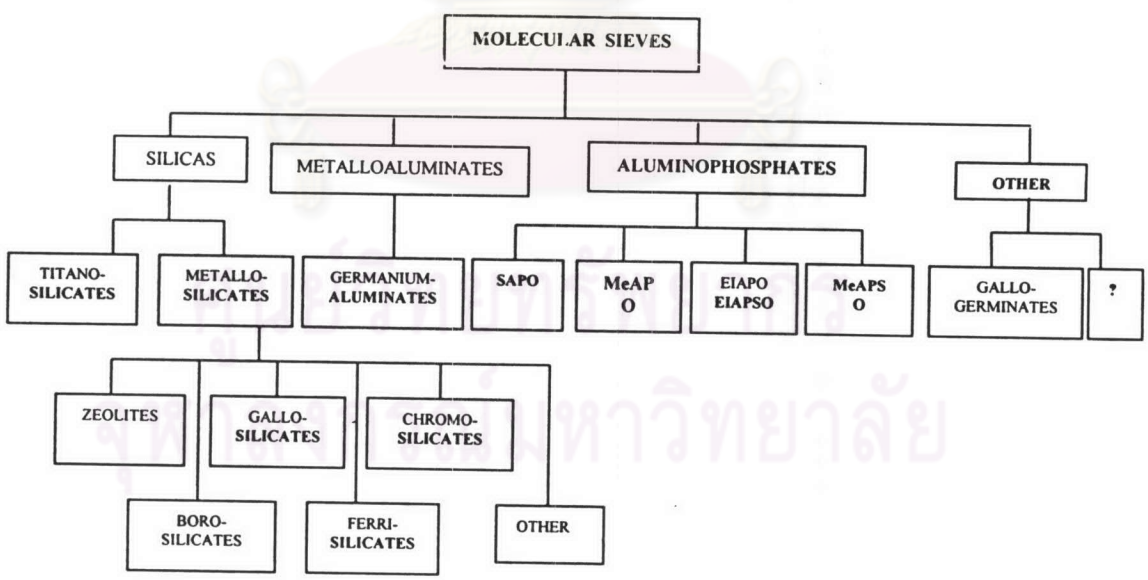

Figure 2.1 Classification of molecular sieve materials indicating the extensive variation in composition.[38]

According to the IUPAC classification,[16] molecular sieves can be classfied into three main categories as shown in Table 2.1.

Table 2.1 Classification of porous materials

Class of porous	Pore size (Å)	Examples
Macropores	> 500	glasses
Mesopores	20 - 500	M41S, pillared layered clays
Micropores	< 20	zeolites, activated carbon

2.1.1 Zeolites

Zeolites are crystalline microporous aluminosilicate with a structure based on an extensive three-dimensional framework which formed by connection of tetrahedral $[AlO_4]^5$ and $[SiO_4]^{4-}$ lingkage. The AlO_4^{5-} tetrahedra, or empirically AlO_2^- in the structure determine the framework charge and will be balanced by cations occupied nonframework positions. A representative empirical formula for a zeolite is written as:

$$M_{2/n}O \cdot [Al_2O_3 \cdot xSiO_2] \cdot yH_2O$$

M represents the exchangeable cations, generally from group I or II in the periodic table of element

n represents the cation oxidation state

x is equal to or greater than 2 because Al^{+3} does not occupy adjacent tetrahedral sites.

The framework contains channels and interconnected voids which are occupied by the cation M and water molecules.

The primary building units for aluminosilicate zeolites are the $[SiO_2]^{4-}$ and $[AlO_2]^{5-}$ tetrahedra *i. e.* formally Si^{4+} or Al^{3+} at the center of a tetrahedron with O_2^- at each apex as shown in Figure 2.2. The trahedra are corner shared to form ordered three-dimensional macrostructures. Zeolite framework structures are usually represented by joining the tetrahedral centers (T) with straight lines, and ignoring the O atoms between the centers.

Figure 2.2 A primary building unit of zeolites.

The combination of high internal surface area, strong acid sites, selective sorption and molecular sieving properties makes the zeolites the most useful among versatile heterogeneous catalysts. High internal surface area and acidity give rise to high activity, while selective sorption and molecular sieving result in high reaction selectivity. Reaction selectivity may be diffusionally controlled (reactant or product selectivity) or may be geometrically controlled (transition state selectivity).[15] Figure 2.3 shows the models for the three types of selectivity obseved in zeolites.

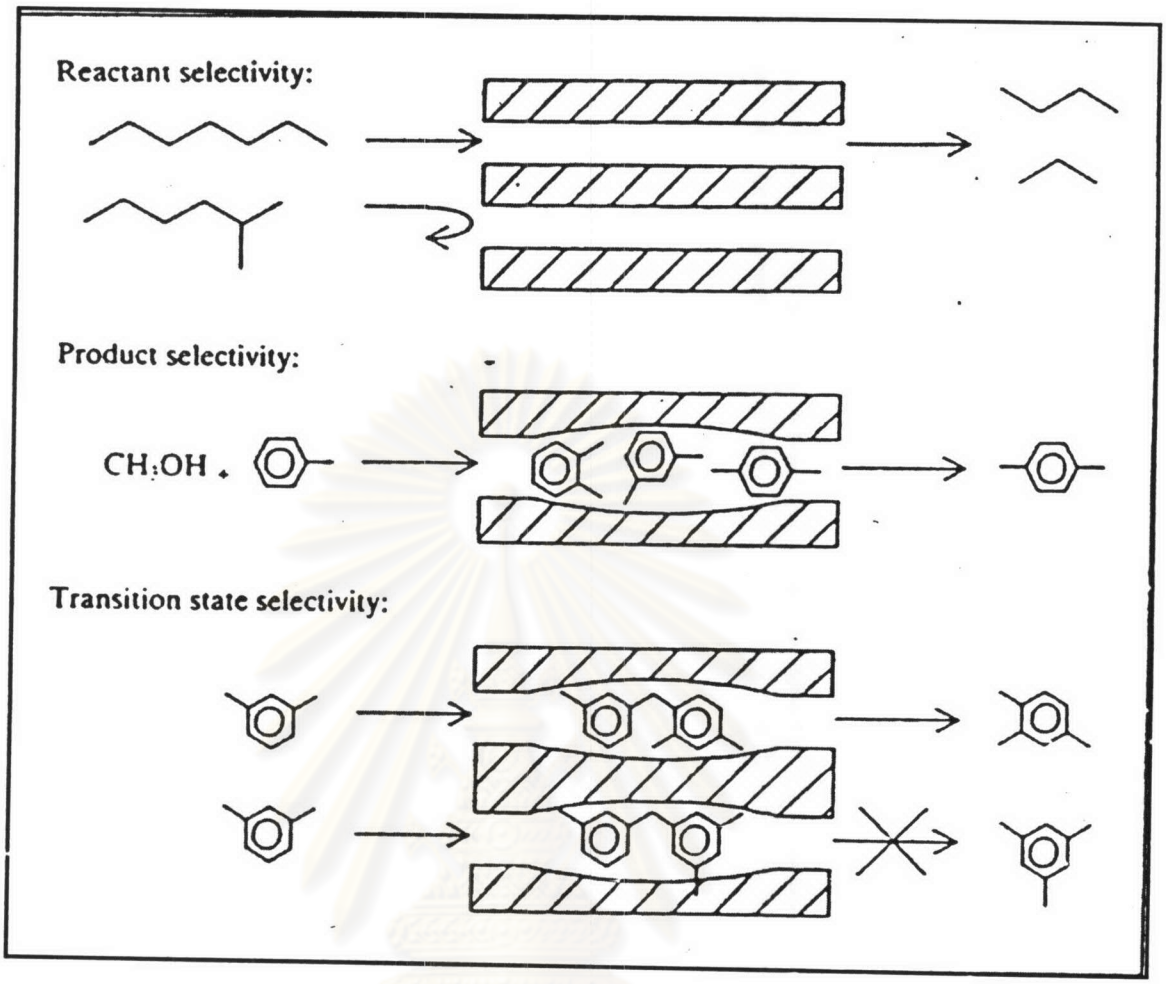

Figure 2.3 Diagram depicting three types of selectivity: reactant, product and transition-state shape selectivity.[38]

2.1.2 Mesoporous Materials

Two classes of meterials that are used extensively as heterogeneous catalysts and adsorption media are microporous and mesoporous materials. Well-known members of the microporous class are zeolites, which provide excellent catalytic properties by the virtue of their crystalline aluminosilicate framework. However, their applications are limited by the relatively small pore openings, although many attemptes to synthesize zeolites with larger pores have been made,

these attempts have been unsuccessful. Larger pores are present in porous glasses and porous gels, which were known as mesoporous materials.

In 1992, Mobil scientists[17] firstly reported the synthesis of mesoporous silicate molecular sieves (M41S). These mesoporous silicate materials are well-defined pore sizes of 15-100 Å, which can break to part of the pore-size constraint (<15 Å) of microporous zeolites. The extremely high surface areas of greater than 1,000 m^2/g and the precise tuning of pore sizes are among the many desirable properties that have made such materials the focus of great interest. The M41S family is classified into several members[39] : MCM-41, MCM-48 and MCM-50. MCM-41 has a hexagonally packed array of noninterconnecting cylindrical pores. The structure of MCM-48 is the cubic and it can be thought of as two intertwined networks of spherical cages separated by a continuous silicate framework. MCM-50 contains a lamellar structure as illustrated in Figure 2.4.

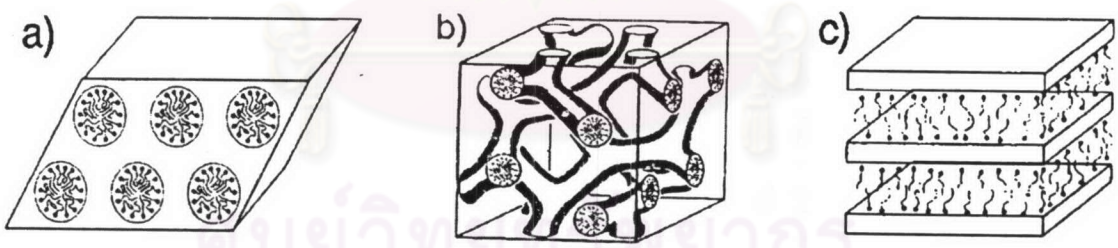

Figure 2.4 Illustration of mesoporous M41S materials : (a) hexagonal MCM-41, (b) cubic MCM-48 and (c) lamellar MCM-50.[39]

2.1.2.1. MCM-41

MCM (Mobil Composition of Matter)[17] 41, a member of the extensive family of mesoporous molecular sieves, has a honeycomb structure that is the result of hexagonal packing of unidimensional cylindrical pores as shown in Figure 2.5.

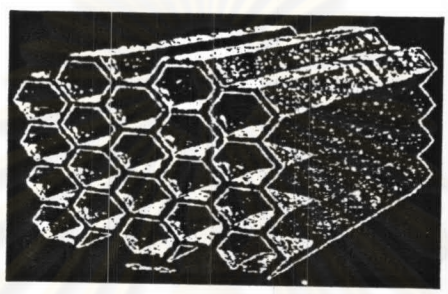

Figure 2.5 Hexagonal packing of unidimensional cylindrical pores.[17]

Reliable characterization of the porous hexagonal structure requires the use of three independent techniques: [17]

(a) X-ray powder diffraction (XRD)

(b) Transmission electron microscopy (TEM)

(c) Adsorption analysis

The XRD pattern of MCM-41 shows typically three to five reflections of two theta (2θ) between 2° and 5°. The reflections are due to the ordered hexagonal array of parallel silica tubes and can be assigned to the coresponding lattice planes of Miller indices (100), (110), (200), (210) and (300). Since the materials are not crystalline at the atomic level, no reflections at higher angles are observed. The wall thickness can be calculated by determining the difference between the lattice parameter ($a = 2d_{100}/\sqrt{3}$). From Bragg's law, when an X-ray beam strikes a crystal surface at some angle θ, a portion is scattered by the layer

of atoms at the surface. The unscattered portion of the beam penetrates to the second layer of atoms[40] as shown in Figure 2.6, where *d* is the interplanar distance of the crystal. Thus, the conditions for constructive interference of the beam at angle θ are called the Bragg equation which is written as Equation (2.1).

$$n\lambda = 2d \sin\theta \qquad (2.1)$$

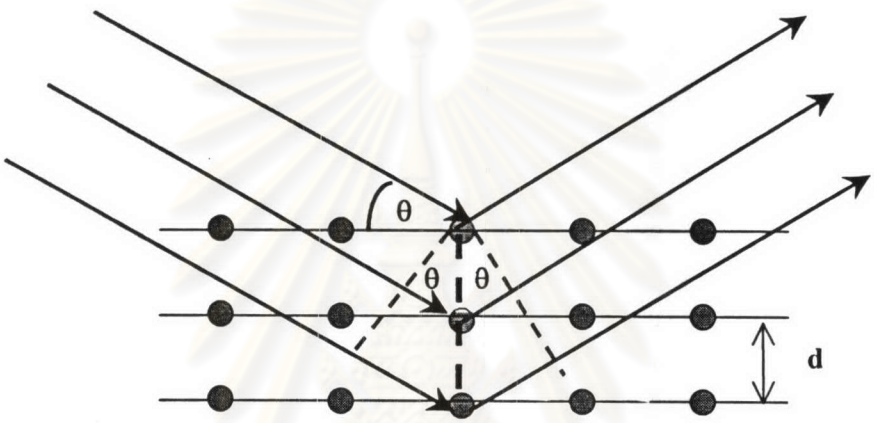

Figure 2.6 Diffraction of X-ray by a crystal.[40]

Hexagonal structure have characteristics of d-spacing ratio as follows :

$$d_{100}/d_{110} = d_{200}/d_{220} = 1.732 = \sqrt{3} \qquad (2.2)$$

$$d_{100}/d_{200} = d_{200}/d_{400} = 2.000 \qquad (2.3)$$

$$\frac{1}{d^2} = \frac{h}{a^2} + \frac{k^2}{b^2} + \frac{l^2}{c^2} \qquad (2.4)$$

From Equation (2.2), (2.3), and (2.4)

$$a = 2d_{100}/\sqrt{3}$$

To elucidate the pore structure of MCM-41, transmission electron microscopy is usually used. Figure 2.7 shows a TEM image of the hexagonal arrangment of uniform, 4 nm sized pores in a sample of MCM-41. The hexagonal

morphology of MCM-41 can be easily observed in SEM as Figure 2.8 if the sample is convertionally prepared.

Figure 2.7 Transmission electron micrograph of MCM-41.[18]

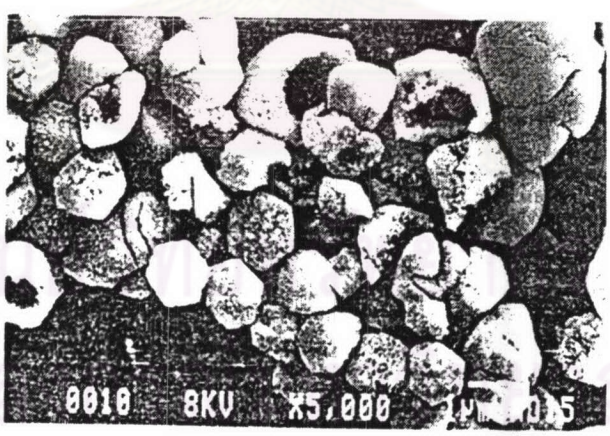

Figure 2.8 Scanning electron micrograph of a MCM-41 sample.[18]

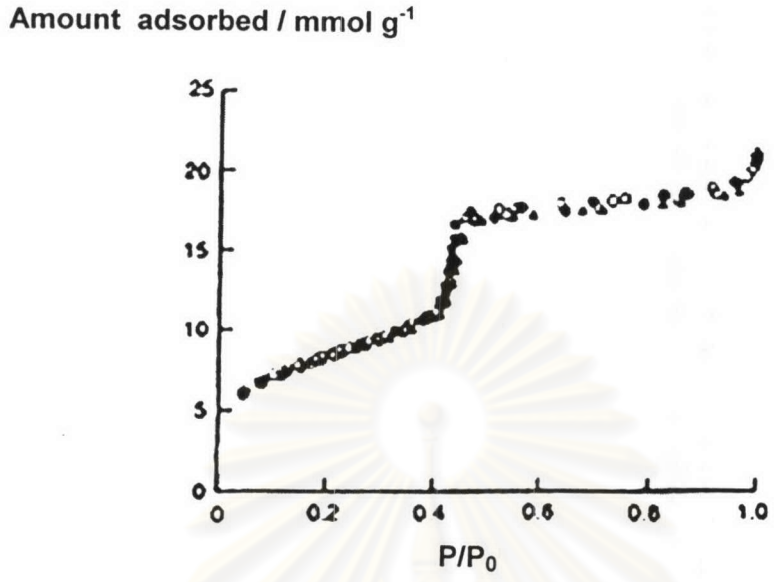

Figure 2.9 Adsorption isotherm of nitrogen on MCM-41 with 4.0 nm pores at -196°C.[17]

Adsorption of probe molecules has been widely used to determine the surface area and to characterize the pore-size distribution of solid catalysts. From Figure 2.9, the nitrogen adsorption isotherm for MCM-41 with pores of around 4.0 nm,which is type IV in the IUPAC classifation, shows two distinct features: a sharp capillary condensation step at a relative pressure of 0.4 and no hysteresis between the adsorption and desorption branches. The adsorption at very low relative pressure, p/p_0, represents the monolayer adsorption of N_2 on the walls of the mesopores and does not imply the presence of any micropores.

2.2 Mechanism for Formation of MCM-41 Structure

2.2.1 Liquid Crystal Templating Mechanism

The original MCM-41 synthesis was carrried out in water under alkaline conditions similar to zeolite syntheses, organic molecules (surfactants) functioned as templates forming an ordered organic–inorganic composite material. Via calcination the surfactant is removed, leaving the porous silicate framework. In contrast to zeolites, the templates are not single organic molecules but liquid–crystalline self–assembled surfactant molecules. The formation of the inorganic–organic composite is based on electrostatic interactions between the positively charged surfactants and the negatively charged silicate species. Beck *et al.*[16] suggested a "liquid crystal templating (LCT)" mechanism for the formation of the M41S materials as shown in Figure 2.10.

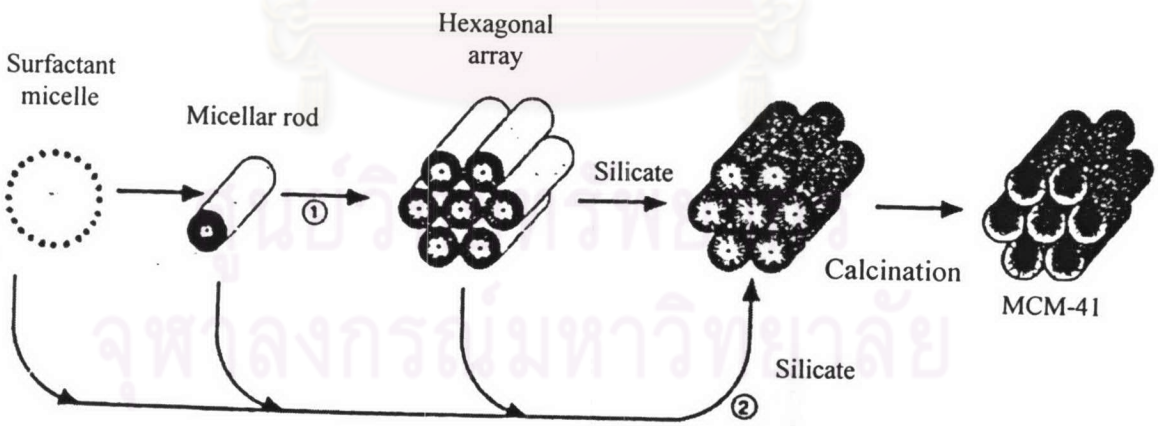

Figure 2.10 Two possible pathways for the LCT mechanism.[16]

There were two main pathways, in which either the liquid–crystal phase was intact before the silicate species were added (pathway 1), or the addition of the silicate results in the ordering of the subsequent silicate–encased surfactant micelles (pathway 2). In this mechanism, inorganic material occupied the solvent (water) region to create inorganic walls between the surfactant cylinders. It might be that encapsulation occurred because anionic silicate species entered the solvent region to balance the cationic hydrophilic surfaces of the micelles. Alternatively, it might be the introduction of the silicate species themselves that mediated the hexagonal ordering. Once an ordered array was established, subsequent thermal processing was used to remove the organic material and produced a stable mesoporous molecular sieve. The second mechanistic pathway of LCT was vaguely postulated as a cooperative self-assembly of the ammonium surfactant and the silicate precursor species below the critical micelle concentration (CMC). It has been known that no preformed liquid crystal phase was necessary for MCM-41 formation but, to date, the actual details of MCM-41 formation have not yet been fully agreed upon. Several mechanistic models have been advanced which share the basic idea that the silicate species promoted the liquid crystal LC phase formation below the CMC.

2.2.2 Silicate-Encapsulated Rods

Davis *et al.*[41] found that the hexagonal liquid crystal phase did not develop during MCM-41 synthesis. They proposed that, under the synthesis conditions reported by Mobil, the formation of MCM-41 began with the deposition of two to three monolayers of the silicate precursor onto isolated surfactant micellar rods as shown in Figure 2.11. The silicate-encapsulated rods were randomly ordered, eventually packing into a hexagonal mesostructure. Heating and aging then

completed the condensation of the silicates into the as-synthesized MCM-41 mesostructure.

Figure 2.11. Assembly of silicate-encapsulated rods proposed by Davis *et al.*[41]

2.2.3 Silicate Layer Puckering

Instead of the formation of silicate-covered micellar rods, Steel *et al.*,[42] postulated that surfactant molecules assembled directly into the hexagonal liquid crystal phase upon addition of the silicate species, based on ^{14}N-NMR spectoscopy. The silicates were organized into layers, with rows of the cylindrical rods intercalated between the layers as illustrated in Figure 2.12. Aging the mixture caused the layers to pucker and collapse around the rods, which then transformed into the surfactant-containing MCM-41 hexagonal-phase mesostructure.

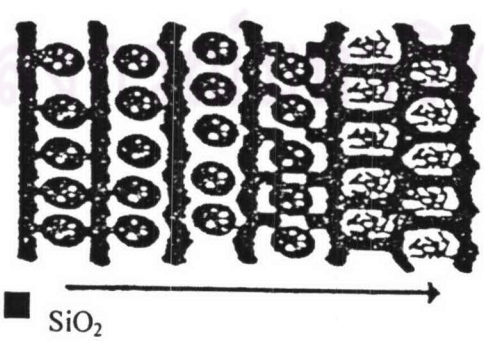

Figure 2.12. Puckering of silicate layers in the direction shown.[42]

2.2.4 Charge Density Matching

A "charge density matching" mechanistic model, proposed by Monnier *et al.*[43] suggested that MCM-41 could be derived from a lamellar phase. The initial phase of the synthesis mixture was layered as detected by X-ray diffractometry, and was formed from the electrostatic attraction between the anionic silicates and the cationic surfactant head groups as depicted in Figure 2.13. As the silicate species began to condense, the charge density was reduced. Accompanying this process, curvature was introduced into layers to maintain the charge density balance with the surfactant head groups, which transformed the lamellar mesostructure into the hexagonal mesostructure.

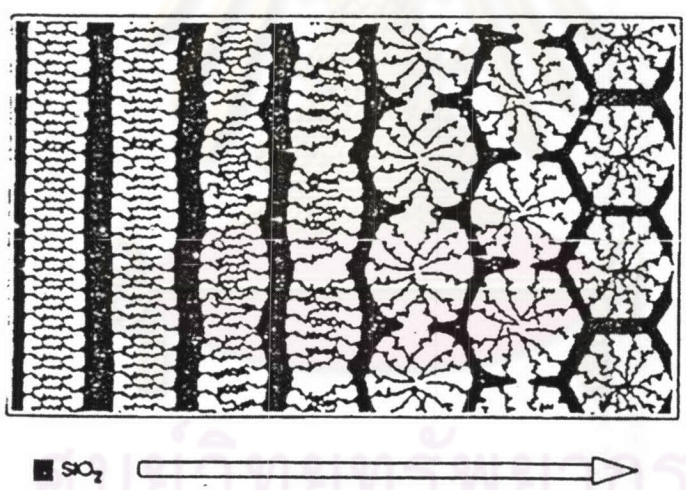

Figure 2.13. Curvature induced by charge density matching. The arrow indicates the reaction coordinate.[43]

2.2.5 Silicatropic Liquid Crystals

Under synthesis conditions that prevented condensation of the silicate species, such as low temperatures and high pH (*ca.* 14), a true cooperative self-

assembly of the silicates and surfactants was found possible, Firouzi *et al.*[44] A micellar solution of cetyltrimethylammoniumbromide (CTAB) transformed to a hexagonal phase in the presence of silicate anions. The silicate anions ion-exchanged with the surfactant halide counterions, to form a "silicatropic liquid crystal" (SLC) phase as illustrated in Figure 2.14. The SLC phase exhibited behavior very similar to typical lyotropic systems, except that the surfactant concentrations were much lower and the silicate counterions were reactive. Heating the SLC phase caused the silicates to condense irreversibly into MCM-41.

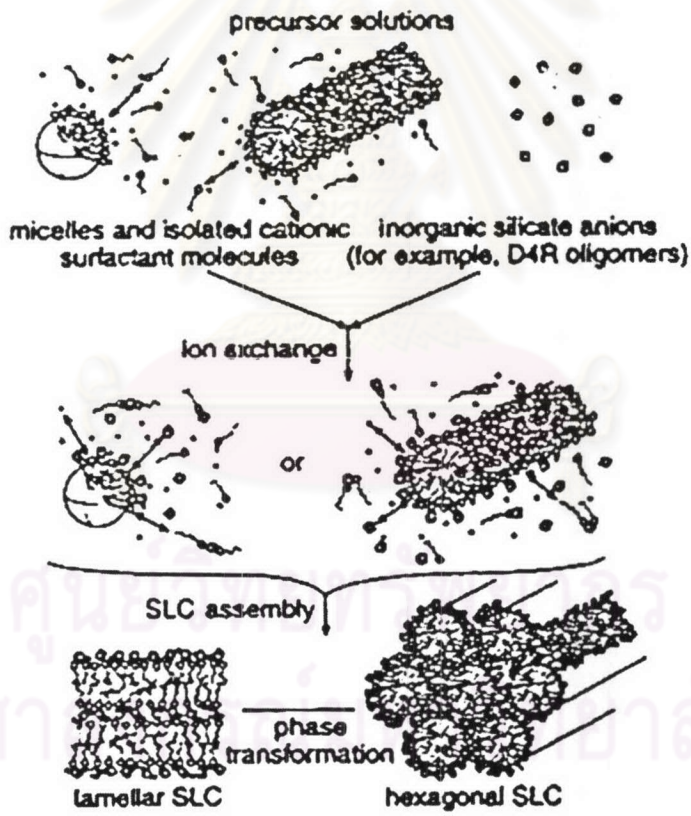

Figure 2.14. Formation of a silicatropic liquid crystal phase.[44]

2.2.6 Silicate Rod Clusters

Regev *et al.*[45] found that MCM-41 might be formed heterogeneously, MCM-41 intermediate structures in the form of clusters of rodlike micelles wrapped by a coating of silicate through low-temperature transmission electron microscopy and X-ray scttering. The clusters of elongated micelles were found before precipitation occurred. The silicate species diffused to and deposited onto the individual surfaces of the micelles within the cluster and the clusters of elongated micelles eventually became clusters of silicate-covered micelles. Thus, the clusters of micelles served as nucleation sites for MCM-41 formation.

2.2.7 Generalized Liquid Crystal Templating Mechanism Electrostatic Interaction

A generalized LCT mechanism of MCM-41 is based on formation[45] based on the specific type of electrostatic interaction between a given inorganic precursor, I, and a surfactant head group, S. The pathway 2 of the original LCT mechanism as illustrated in Figure 2.10, which involved anionic silicate species and cationic quaternary ammonium surfactant, could be categorized as the S^+I^- pathway. By extension, the other charge-interaction pathways are S^-I^+, $S^+X^-I^+$ (X^- is a counteranion), and $S^-M^+I^-$ (M^+ is a metal cation) as shown in Figure 2.15. The success of the cooperative templating model, referred to here the generalized LCT mechanism in Figure 2.16, was illustrated by the possible diverse compositions of organic-inorganic mesostructures.

The formation mechanisms of the mesoporous silica in acid and alkaline conditions[46] can be compared schematically in Figure 2.17. Using tetraethyl orthosilicate as a silicon source, both mechanisms include a variety of phenomena :

binding of the counterion and surfactant; the hydrolysis of TEOS; preferred polymerization of silicate species at the surfactant-silicate interface; and charge-matching combination of the surfactant and silicate oligomers. The primary distinction of the two formation processes is in the cooperative interaction between surfactant and silica species. In alkaline condition, the silica species are negatively charged and thus energetically favored to condense at the surface of the positive charged surfactant (S^+) through the strong electrostatic interactions (S^+I^-). Thus the addition of couterion (X^-) with stronger binding affinity would decrease the number of active sites (S^+). In acid synthesis (pH<1), the dominating cationic silica precursor (I^+) combines with S^+X^- type active sites on the surfactant micelles through a weaker electrostatic interactions. To promote the silica condensation in $S^+X^-I^+$ without releasing X^-. Therefore, the counterion effect in the alkaline synthesis is opposite to the acidic synthesis.

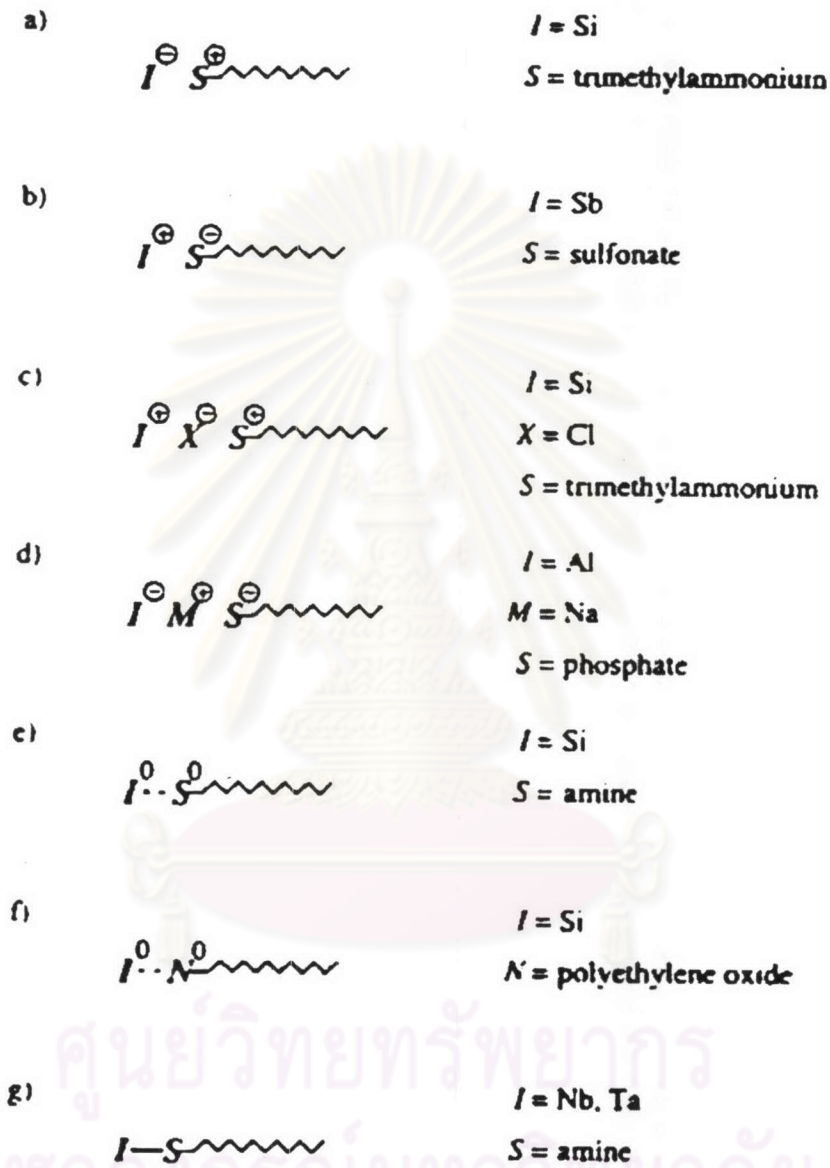

Figure 2.15 Schematic representation of various types of inorganic surfactant head group interactions : electrostatic: a) S^+I^-, b) S^-I^+, c) $S^+X^-I^+$, and d) $S^-M^+I^-$; hydrogen bonding : e) S°I° and f) N°I°; and covalent bonding: g) S^-.[45]

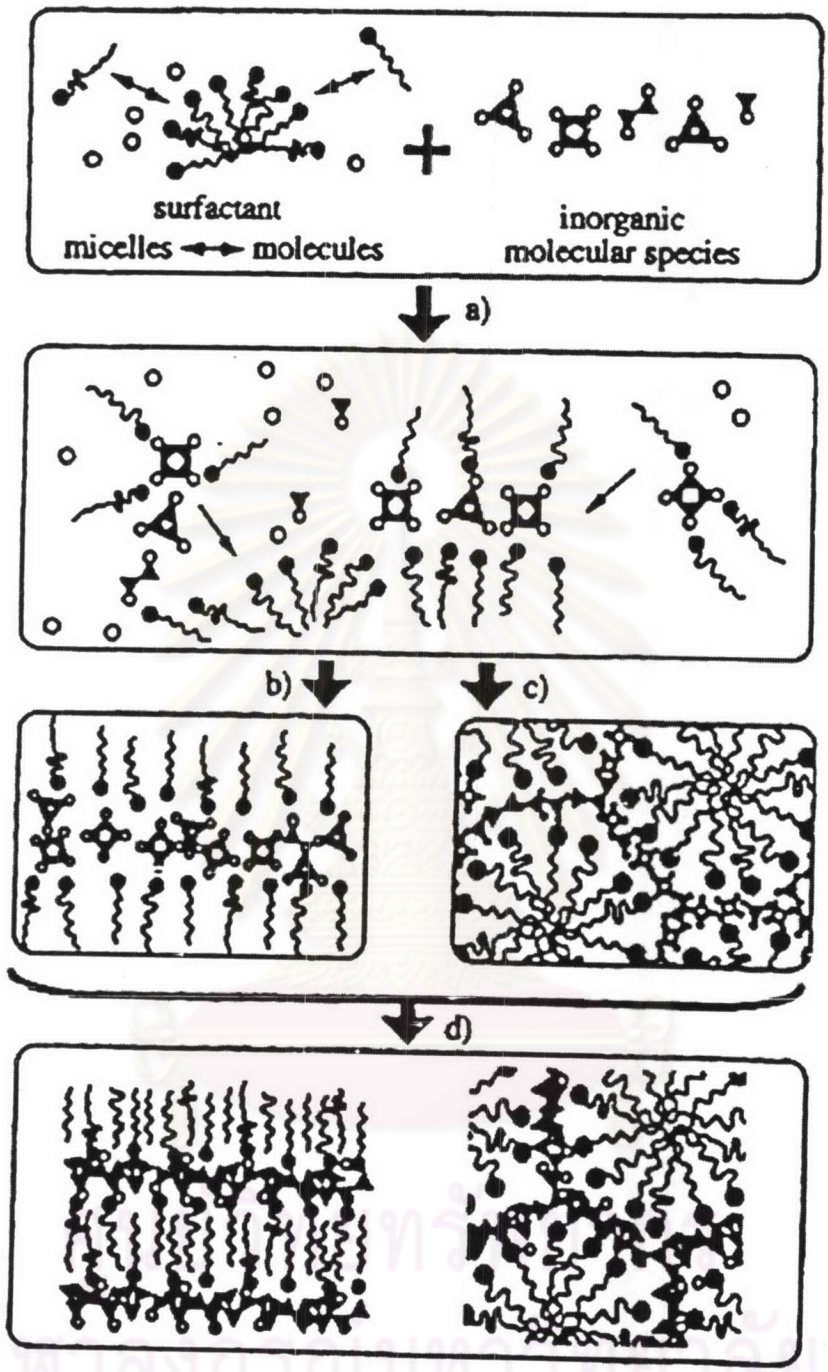

Figure 2.16 Cooperative templating of the generalized LCT mechanism: a) cooperative nucleation; b), c) liquid crystal formation with molecular inorganic compounds; d) inorganic polymerization and condensation.[45]

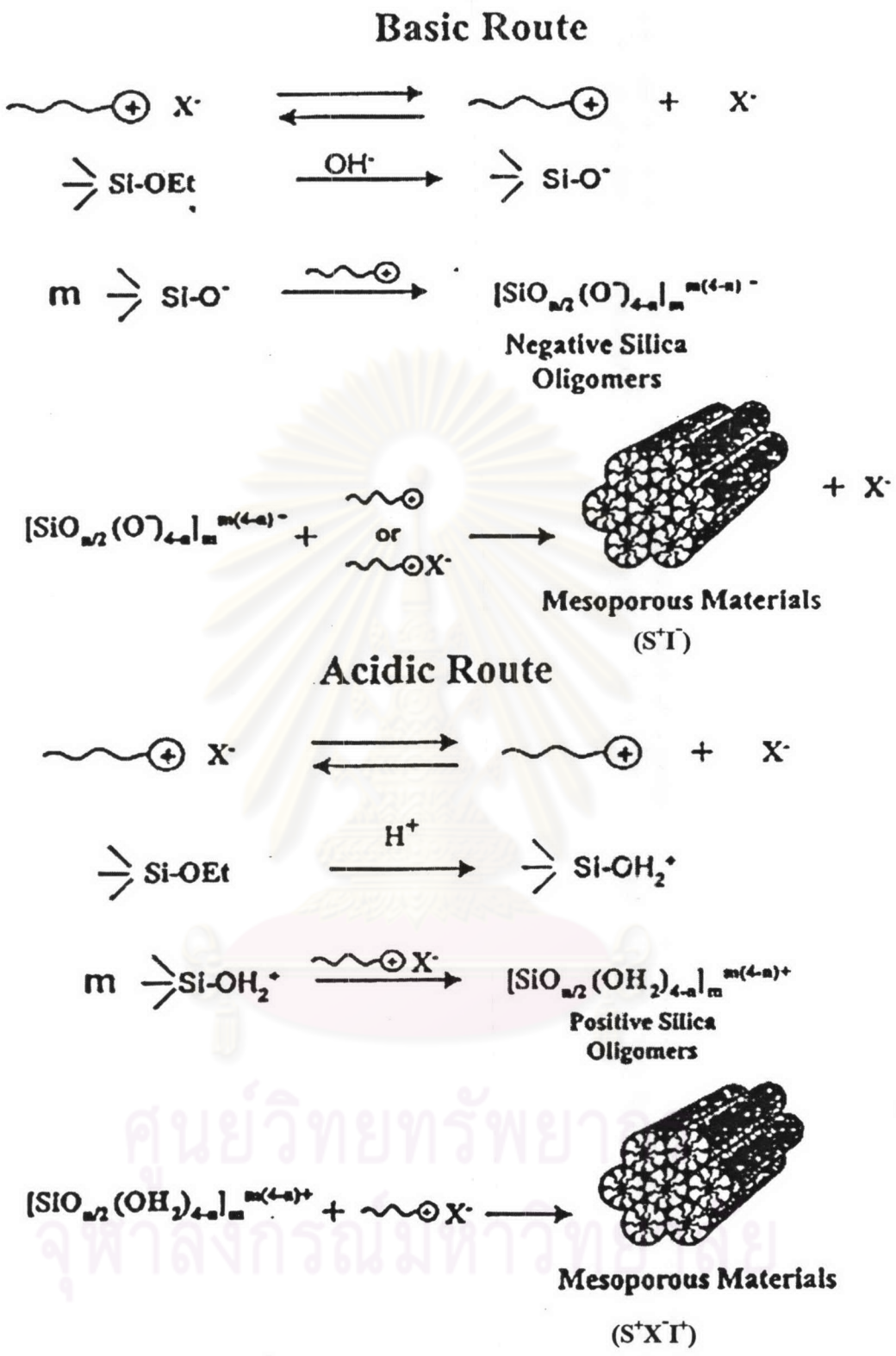

Figure 2.17 The comparison of the formation processes of the mesoporous materials in basic and acidic conditions.[46]

2.3 Effect of Parameters on the MCM-41 Synthesis

2.3.1 Surfactant

Surfactant plays an important role in the synthesis of MCM-41 such as pore size, and structure. It has been reported that MCM-41 pore diameter generally increases with increasing surfactant chain length. When quaternary ammonium surfactants ($C_nH_{2n+1}(CH_3)_3N^+$) with different alkyl chain lengths[16] (n = 8-16) were used, MCM-41 materials obtained exhibit XRD d-spacings as shown in Table 2.2.

Table 2.2. Effect of surfactant chain length on MCM-41 pore size, XRD d_{100} peak location, hexagonal unit cell parameter ($a = 2d_{100}/\sqrt{3}$)

Surfactant chain length, (n) in $C_nH_{2n+1}(CH_3)_3N^+$	XRD d_{100} d-spacing (Å)	Unit cell parameter, a (Å)	Average pore size (Å)
8	27	31	18
9	28	32	21
10	29	33	22
12	29	33	22
14	33	38	30
16	35	40	37

Furthermore, Vartuli *et al.*[47] found that the surfactant/silicon molar ratio was the key parameter for controlling the mesophase structure. The result was concluded in Table 2.3. The MCM-41 was obtained only when the molar ratio of surfactant and silicon less than 1.

Table 2.3. Mesophases of silicate molecular sieves and controlling synthesis parameters

Name	Mesophase	[Surfactant]/[Si]
MCM-41	Hexagonal	<1
MCM-48	Cubic	1-1.5
MCM-50	lamellar	1.2-2

2.3.2 pH

Tatsumi *et al.*[48] inverstigated the effect of TMAOH on the Ti-MCM-41 structure with the gel composition of 1TEOS : 0.01 TBOT : 0.6 DTMABr : 0.3 TMAOH : $60H_2O$ by measuring pH before the hydrothermal treatment. They reported that the optimum pH for the hexagonal phase was in the range of 11-12. The pH lower than 11 resulted in the formation of amorphous materials. At the higher pH (11.5-12), highly crystalline hexagonal phase was obtained with relatively low yield and no solid product was found at pH higher than 12.

A hydrothermal procedure with pH adjustment has been develped in order to obtain MCM-41 of high structural order. Figure 2.18 shows XRD patterns of the MCM-41 mesostructure with molar gel composition of 4 SiO_2 : 1 HTACl : 1 Na_2O : 0.15 $(NH_4)_2O$: $200H_2O$) at various conditions.[49] The structure formed at room temperature had a relatively low diffraction intensity and resolution, while the structure obtained after heating the reaction mixture at 373 K for one day exhibited four Bragg

diffraction peaks with high resolution and intensity. It was suggested that the structure obtained from low temperature had a large number of excess silanol groups due to a low degree of silicate cross-linking in the framework. The excess silanol groups were condensed during calcination, leading to the loss of the structural order. The pH adjustment and heating could prevent the loss of structural orders. The effect resulting from the pH adjustment during the hydrothermal synthesis, was attributed to shift the reaction equilibrium toward the silicate condensation while the framework was supported by the surfactant. Five well-resolved XRD peaks were obtained for the pure-silica MCM-41 sample synthesized by three-times repeating pH adjustment and heating alternately.

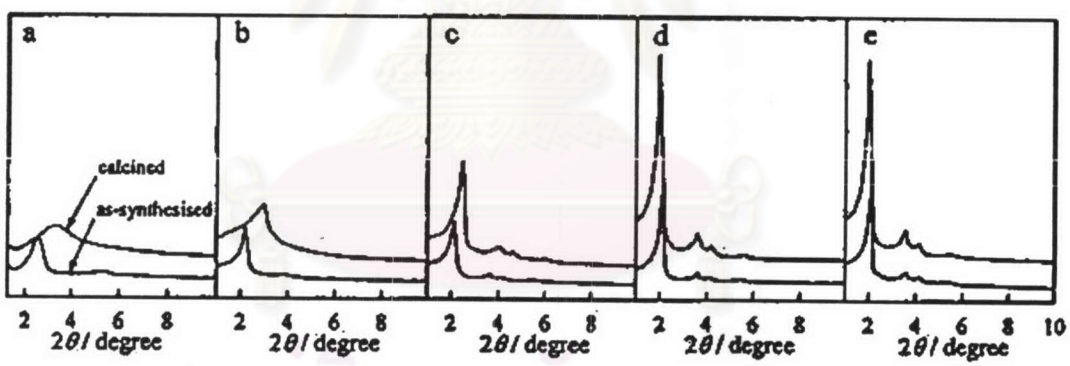

Figure 2.18 XRD patterns of MCM-41 syntehsized (a) at room temperature for 5 h, and at 373 K (b) without pH adjustment, (c) with pH adjustment to 10, (d) by repeating pH adjustment twice, and (e) three times.[49]

2.4 W-MCM-41

Tungsten oxides are versatile composite which has been extensively used as catalysts for hydrodesulfurization, hydroxylation of unsaturated organics and alkene metathesis. The preparation of tungstenoxides on amorphous support has been well known, but only few publications were reported for the incoporated tungsten into the ordered MCM-41 structure. In 1999, Zhang *et al.* [50,51] reported the synthesis of novel tungsten-containing MCM-41 so called W-MCM-41 and oxidation reaction of cycloalkene with H_2O_2. The long-range-ordered W-MCM-41 was directly synthesized by hydrolysis of tetraethyl orthosilicate and ammonium tungstate via the halogen anion mediated $S^+X^-I^+$ assembly using cetylpyridinium bromide (CPBr) as a template in a strongly acidic medium. The gel compostion was TEOS : 0-0.033 W : 0.3CPBr : 6HCl : $60H_2O$. The gel was aged at 50°C under gentle stirring. After 22 hours, the solid product was centrifuged, washed with distilled water, and air-dried. The characterization and analysis results on W-MCM-41 showed that tungsten was incorporated in the tetrahedrally coordinate positions of the MCM-41 framework when its general content in the mesophase did not exceed ca. 5.6% ($Si/W \geq 50$). Furthermore, the catalytic test suggested that the isolated W sites incorporated in the framework of MCM-41, showed high catalytic activity on the hydroxylation rate of cyclohexene without decreasing the *trans*-cyclohexane-1,2-diol yields, compared to the crystallite WO_3. The hydroxylation of cyclohexene were performed using dilute H_2O_2 as an oxidant and acetic acid as a solvent.

On the contrary, the synthesis of a tungsten-containg MCM-41 in a strongly acidic media may involve oligomeric species of WO_3 upon the calcination and it is not easy to reproduce the synthesis method.

2.5 Impregnation

Impregnation[52,53] is the easiest method of making a heterogeneous catalyst. A support or carrier, usually a porous material will be in contacted with a solution of one or more suitable metallic compounds. The carrier is then dried, and the catalyst is activated as in case of precipitated catalysts. The size and shape of the catalyst particles are those of the carrier. The impregnation technique requires less equipment since the filtering and forming steps are eliminated and washing may not be needed. It is the economically desirable method in preparing supported noble metal catalysts in order to spread out the metal in a highly dispersed form as possible. The noble metal is usually present in the order of 1% by weight. or less of the total. This makes maximum use of a very expensive ingredient; in contrast, in a precipitated catalysts some of the active ingredient will usually be enclosed by other material present and thus unavailabie for reaction.

Impregnation method can be divided into two types;

(a) Wet Impregnation

This method can be prepared by adding an excess amount of metal salt solution into supports. The composition of the solution will be changed slowly as the metal is absorbed on the surface. Thus, the metal content on the support will not be equal to the initial content in the solution. Besides, the release of support debris in the solution might form a mud, which makes it difficult to separate from the catalyst.

(b) Dry Impregnation or Impregnation to incipient wetness

This method is favored for industrial catalysts because the solution of metal salt will be dispersed by spraying on supports. The volume of solution should be equal to the pore volume of support in order to control the amount of active component. The required catalyst was obtained after drying and calcination step.

2.6 Olefin Metathesis

2.6.1 Definition of Olefin Metathesis

Olefin Metathesis[27,54,55] or olefin disproportionation reaction is an exchange reaction between two olefins in which alkylidene groups are interchanged (transalkylidenation reaction) at the double bond. Each half of one olefin can become attached to either half of the other olefin. The general form of olefin metathesis reactions is shown in Equation 2.5.

$$\begin{matrix} R^1CH{=}CHR^2 \\ + \\ R^3CH{=}CHR^4 \end{matrix} \rightleftharpoons \begin{matrix} R^1CH{=}CHR^3 \\ + \\ R^2H{=}CHR^4 \end{matrix} \rightleftharpoons \begin{matrix} R^1CH{=}CHR^4 \\ + \\ R^2CH{=}CHR^3 \end{matrix} \qquad (2.5)$$

An initial pair of olefins in which $R^1 \neq R^2 \neq R^3 \neq R^4$ may produce six different combinations of alkylidene units, but olefins with more than one substituent per carbon are comparatively rare. Olefin used in the metathesis process are acyclic monoenes and polyenes having at least 3 carbon atoms per molecule including cycloalkyl and aryl derivatives, cyclic monoenes and polyenes having at least 4 carbon atoms per molecule including alkyl and aryl derivatives, mixtures of the above olefins, and mixtures of ethylene and the above olefins. Many useful reactions are accomplished with such acyclic olefins having 3-30 carbon atoms per molecule and cyclic olefins having 4-30 carbon atoms per molecule. Different types of monoolefin and diolefin undergo metathesis via contact with a suitable catalyst, resulting in a wide variety of possible products[6] as shown in Equations 2.6 to 2.9.

Acyclic olefins

(2.6)

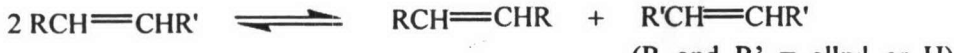

Diolefins

Intermolecular Reaction

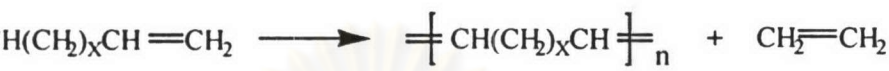

(2.7)

Intramolecular Reaction

(2.8)

Cyclic Olefins

(2.9)

(where ( ) represents a hydrocarbon chain with or without a heteroatom)

Diolefins, such as α,ω-dienes, undergo intermolecular and intramolecular metathesis. Intermolecular reactions, as shown in Equation 2.7, eventually lead to the production of high polymers, known as acyclic diene metathesis (ADMET) polymers. If the diolefin couples undergo intramolecular to produce a cyclic alkene, as shown in Equation 2.8, the process is called ring-closure metathesis (RCM). RCM has become an important tool for organic synthesis and has been widely applied for the preparation of carbocyclic and heterocyclic intermediates. The reverse reaction of RCM is called ring opening cross-metathesis. Equation 2.9 is an example of ring-opening metathesis polymerization (ROMP). The reaction is driven by the release of ring strain of the starting cycloalkene. Living polymerization occurs when the metal carbene

catalyst reacts more rapidly with the cyclic olefin than those with a C=C bond of the growing polymer chain. All double bonds from monomer molecules are preserved in ROMP, resulting in the formation of polymers with highly unsaturated backbones.

Metathesis reactions of acyclic mono-olefins[56] can be classified into two groups: (1) a self-metathesis of a single olefin, and (2) a cross-metathesis of double-bond isomers of two different olefins. The self-metathesis reaction occurs between a pair of molecules of two original unsymmetric olefins in order to produce a pair of symmetric olefins; for example, $R^1CH=CHR^2$ produces $R^1CH=CHR^1$ and $R^2CH=CHR^2$, and $R^3CH=CHR^4$ gives $R^3CH=CHR^3$ and $R^4CH=CHR^4$. Thus, in the self-metathesis reaction, four symmetric combinations of alkylidene units are added to six unsymmetric combinations produced by Equation 2.5. The initial pair of olefins may become a mixture of twenty different olefins. Thus, the reactions must be designed for an appropriate use. If it starts with a single olefin, only self-metathesis is possible and the number of combinations will be small. If a terminal olefin is prefered as in Equation 2.10, the situation is even simpler because the reaction can be completed in either direction. For example, the removal of ethylene drives equilibrium in Equation 2.11 to the right; therefore, 1-pentene can be converted to 4-octene in good yields. Conversely, excess ethylene drives equilibrium in Equation 2.12 to the left, thus, stilbene can be converted to styrene. These reactions are useful ways for producing terminal olefins from symmetric internal olefins.

$$2RCH{=}CH_2 \rightleftharpoons RCH{=}CHR + CH_2{=}CH_2 \qquad (2.10)$$

$$2PrCH{=}CH_2 \longrightarrow PrCH{=}CHPr + CH_2{=}CH_2 \qquad (2.11)$$

$$2PhCH{=}CH_2 \longleftarrow PhCH{=}CHPh + CH_2{=}CH_2 \qquad (2.12)$$

Metathesis reaction can be distinguished into three different types:[57] (1) the productive metathesis yielding new products, (2) the degenerate or non-productive metathesis, in which the exchange of alkylidene groups does not result in new products, and (3) the cis-trans isomerisation. For metathesis of asymmetric internal alkenes, these reactions occur simultaneously while in the metathesis of 1-alkenes only the first two reactions occur.

2.6.2 Olefin Metathesis Mechanism

Generally, the metathesis reaction involves a simultaneous cleavage of double bonds of two olefins followed by the formation of alternate double bonds[58] as shown in Equation (2.13),

$$C{=}C + \overset{*}{C}{=}\overset{*}{C} \xrightarrow{M} 2\overset{*}{C}{=}C \qquad (2.13)$$

where M is an appropriate metal complex. The Chauvin mechanism,[55] first proposed by Herisson and Chauvin in 1970 and now generally accepted, is illustrated in Scheme 2.1 for the initial pair of olefins in metathesis reaction with a carbene catalyst M=CHR. It begins with formation of a metallacyclobutane (I), from the carbene complex and one of the olefin reactants. Fragmentation of I gives a new carbene complex and a new olefin, when the other olefin reactant is added, the new carbene complex forms another metallacyclobutane (II). Fragmentatin of II finally

gives an olefin which does not contain the carbene ligand of the catalyst. This mechanism is continuously operated.

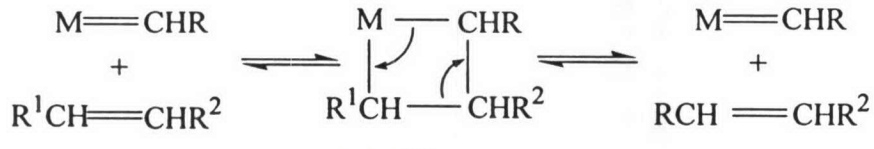

(I)

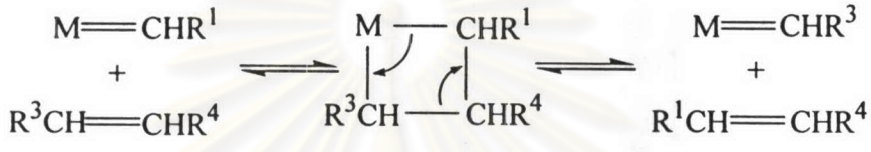

(II)

Scheme 2.1 The Chavin mechanism for olefin metathesis.

There are two general classes of complexes[58] used to mechanistically investigate olefin metathesis : (1) high valent (generally d^0) complexes of Mo, W and Re (these are important industrial catalyst) and (2) low valent complexes of Cr, Mo, and W (oxidation state of zero and these have been significant in determining the general mechanism for the metathesis reaction but are generally not catalytic and industrial important). For example, considering the propylene metathesis mechanism[59] of a mixture between C_3H_6 and C_3D_6, the reaction of C_3D_6 with the catalyst results in the metallocarbenes III and IV.

$M{=}CD_2$ $\qquad$ $M{=}CDCD_3$

III $\qquad$ IV

The addition of propylene to speices III generates a metallacyclobutane, which will be decomposed to either the degenerative or the productive metathesis, depending upon

the orientation of the propylene molecule. The illustration of the degenerative and productive metathesis of propylene by $M{=}CD_2$ are shown in Scheme 2.2. The analogous reactions can also be written for species IV.

Degenerative metathesis :

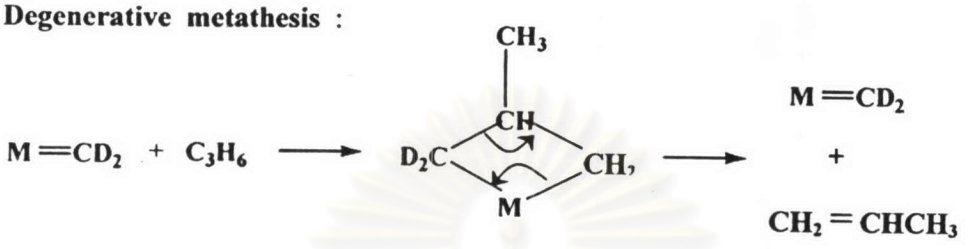

Productive metathesis :

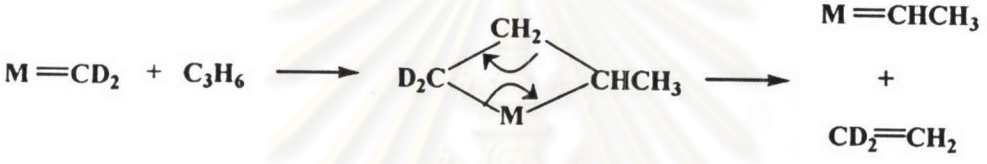

Scheme 2.2 The illustration of the degenerative and productive metathesis of propylene by $M{=}CD_2$.

For example, the mechanism of the molybdenum-containing catalyst which is molybdenum oxide supported on a solid matrix of aluminum oxide or silica, was proposed[60] The catalytically active metal-carbene intermediate was claimed to be formed by the 1,2-hydrogen shift of the alkenyl molybdenum complex and generated a catalytically active species, $Mo{=}CH_2$. That can be expressed as Equation 2.14. The metal carbene proceeded metathesis reaction by the cycle as shown in Scheme 2.3.

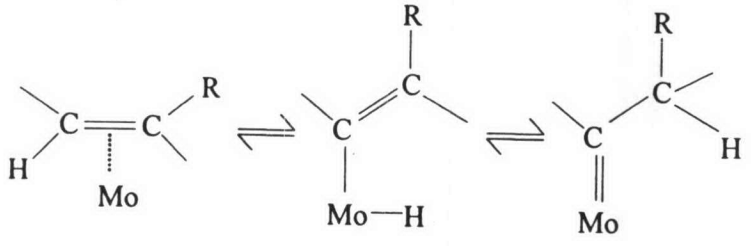

(2.14)

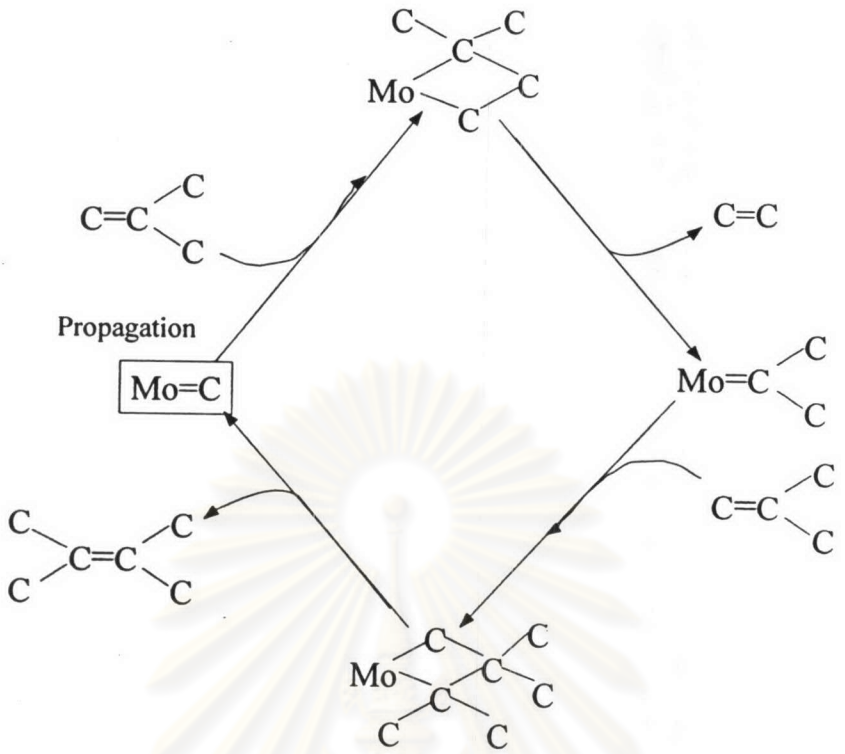

Scheme 2.3 Metathesis reaction cycle.

2.6.3 Olefin Metathesis Catalysts

The metathesis reaction can be catalyzed by both heterogeneous[60] and homogeneous catalysts.[61,62] In homogeneous catalysts, all constituent elements are soluble in a reaction medium, while heterogeneous one will have at least one element insoluble in the reaction medium. These catalysts include a wide range of transition metal compounds, and the most important catalysts are based on molybdenum, tungsten, ruthenium and rhenium.

2.6.3.1 Homogeneous Catalysts

The homogeneous catalysts receiving extensive attention in both academic and industrial laboratories are of three major types. One family might be designated Ziegler Natta catalysts because they are based on combinations of alkyl aluminum, magnesium, or lithium reagents with transition metal chlorides, such as WCl_6 and $WOCl_4$, containing alkylidene metal complexes. The discrete alkylidene complexes of Mo and W have been very effective for the ring-opening metathesis polymerization reactions. The other family is derived from metal carbonyls, expecially $Mo(CO)_6$ and $W(CO)_6$, and ligand-substituted derivatives such as $[W(CO)_5Cl]^-$. The metal carbonyl catalysts usually require the activation by photolysis or by addition of a Lewis acid. Also, the metal carbonyls can be used to prepare heterogeneous catalysts. The other family has been carried out in water with catalysts derived from aquoruthenium (II) ions. This system appears to be closely related to the alcoholic $RuCl_3$ catalyst, which is a major industrial soluble metathesis catalyst used to produce polynorbornene. Examples of homogeneous catalysts are concluded and presented in Table 2.4. The homogeneous catalysts have been extensively used in polymerization reactions (predominantly ROMP) more than metathesis of acyclic alkenes. Access to pure, structurally well-characterized catalysts reduce impurities in polymer products and reactions are normally carried out near ambient temperature. Excellent functional group compatibility of some catalysts brings the metathesis reaction to the organic chemistry synthesis.

Table 2.4. Examples of homogeneous catalysts for olefin metathesis at room temperature.

Catalyst	Ratio	Time	Solvent
$WCl_6/EtAlCl_2/EtOH$	1 : 4 : 1	1-3 min	Benzene
WCl_6/n-BuLi/$AlCl_3$	2 : 4 : 1	15 min	Benzene
$WCl_6/LiAlH_4$	1 : 1	15 min	Chlorobenzene
$MoCl_2(NO)_2(PPh_3)_2/Me_3Al_2Cl_3$	1 : 2	2 h	Chlorobenzene
$ReCl_5/n$-Bu_4Sn	2 : 3	24 h	Chlorobenzene
$ReCl_5/Et_3Al/O_2$	1 : 4	2 h	Chlorobenzene

2.6.3.2 Heterogeneous Catalysts

The largest industrial applications of olefin metathesis use normally heterogeneous catalysts. The greater thermal stability and the ease of separation of products from catalyst are two major advantages. The heterogeneous metathesis catalysts generally consist of a transition metal oxide (e.g. rhenium, molybdenum, or tungsten oxide) supported on a high surface area inorganic oxide such as alumina, silica or other inert surfaces. The catalysts are usually prepared by impregnation of the support with an aqueous solution of the ammonium salt of the transition metal, then dried in air at 110°C and calcined at temperatures between 500 and 550°C. The reactivity of the reaction is enhanced by the addition of other catalytically active metal derivatives, additives or promoters.

Many heterogeneous metathesis catalysts cannot catalyze the metathesis of functionalized olefins because of their intolerance to functional groups. Interference of the functional groups also reduces the activity of the catalysts, in case, they are active. This increases the costs of the catalyst because much higher catalyst/substrate ratios

must be used than are required for normal olefins. Table 2.5 shows some of the heterogeneous catalysts used for the metathesis of unsaturated carboxylic esters, These esters can be used as test substrates for functionalized olefin metathesis.

Table 2.5 Examples of heterogeneous catalyst systems for the metathesis of unsaturated esters

Catalyst	Substrate[a]	[Ester]/[Metalatom]	T(°C)	t[b](h)	TON
$Re_2O_7/Al_2O_3/Et_4Sn$	MeOl	60	20	2	3
$Re_2O_7/MoO_3/Al_2O_3/Et_4Sn$	MeOl	60	20	2	30
$Re_2O_7/SiO_2\text{-}Al_2O_3/Bu_4Sn$	MeOl	240	40-45	3	120
$Re_2O_7/B_2O_3/SiO_2\text{-}Al_2O_3/Bu_4Sn$	MeUN	350	50	13	348
$CH_3ReO_3/SiO_2\text{-}Al_2O_3$	MeOl[c]	100	25	2	27
$MoCl_5/SiO_2/R_4Sn$	EtOl[d]	110	90	4	99
MoO_3/SiO_2/(CO,hν)/cyclopropane	EtOl	250	50	0.17	125
MoO_3/SiO_2/(CO, laser)/cyclopropane	MeOl	1250	40	3	500

[a]MeOl = methyl oleate ; MeUn = methyl undecenoate ; EtOl = ethyl oleate. [b]Time to reach the highest conversion. [C]Ethenolysis (7 bar). [d]Cross-metathesis with 5-decene.